BACKGROUND ELIMINATION METHODS FOR MULTIDIMENSIONAL COINCIDENCE γ-RAY SPECTRA

MIROSLAV MORHÁČ

Institute of Physics, Slovak Academy of Sciences, Dúbravska cesta 9
Bratislava, 842 28, Slovak republic

and

JÁN KLIMAN, VLADISLAV MATOUŠEK, MARTIN VESELSKÝ, IVAN TURZO
Institute of Physics, Slovak Academy of Sciences,

In the paper new methods to separate useful information from background in one, two, three and multidimensional spectra (histograms) measured in large multidetector γ-ray arrays are derived. The sensitive nonlinear peak clipping algorithm is the basis of the methods for estimation of the background in multidimensional spectra. The derived procedures are simple and therefore have a very low cost in terms of computing time.

1. Introduction

Germanium detectors, because of their high energy resolution, have caused great progress in the study of nuclear structure. Other significant step and renaissance of nuclear spectroscopy, especially in the field of high-spin states, is linked with large multidetector γ-ray arrays. Modern large-volume HPGe γ-ray detectors, equipped with Compton shielding allow to obtain statistically relevant many-fold coincidence experimental data.

Spectrometers as GAMMASPHERE [1], EUROGAM [2], GASP [3] permit to obtain very interesting physical information, especially from heavy ion nuclear reactions, induced or spontaneous fission and others, where high-multiplicity γ -rays are registered. The future progress in the field of nuclear structure understanding depends on our ability to analyze correctly the coincidence data in multidimensional space. Thus, processing of many-fold experimental data deserves special attention.

Analysis is conducted usually by creation two dimensional histograms ($\gamma - \gamma$ coincidence matrices) from double coincidence events, occasionally by creation of three dimensional histograms ($\gamma - \gamma - \gamma$ coincidence cubes) and higher dimension coincidence fields. With help of one, two or several gates, two or more dimensions, the final product - one dimensional projection for given gates is obtained. As the final product in the data processing is the information on energies and intensities of γ -transitions, correct subtraction of background represents a universal problem common for all methods of spectral analysis regardless to how many-fold data are used. Recently, several sophisticated methods have been elaborated [4,5,6,7,8,9,10], which have been incorporated in software packages allowing efficient determination of the requested part of the many-parameter spectrum, created by partial absorption of γ -rays and Compton scattering on detector materials.

Because we work on processing of many-fold data from investigation of prompt γ -ray emission in spontaneous fission of ^{252}Cf, realized on GAMMASPHERE spectrometer, our requirements following from the presence of strong fields of fast neutrons and multiisotopic consistence, i.e., high density of peaks in spectra lead us to develop a new algorithm for elimination of multi-fold background. By development of the new algorithm the following characteristics were required:

- simple and fast algorithm with maximum one free parameter
- efficient algorithm for automatic processing of many-fold data
- sensitivity to Compton edges especially to their contribution to the peak area and to false peaks occurring on intersections of two Compton ridges
- sensitivity to background created in interaction of fast neutrons on isotopes Ge, naturally contained in HPGe detectors.

2. Background estimation algorithm

The aim of the paper is to derive algorithms allowing to separate useless information (background, combinations of coincidences of the background with peaks - ridges) from useful information contained in n-fold coincidence peaks of n-dimensional histogram. The methods are based on Sensitive Nonlinear Iterative Peak clipping algorithm [11].

Before employing SNIP algorithm, in some instances, it can be suitable to apply LLS operator [12]

$$v(i) = \log\left[\log\left(\sqrt{y(i)+1}\ +1\right)\ +1\right] \tag{1}$$

where i represents channel and $y(i)$ are counts in the channel i. The log operator allows to work over a few orders of magnitude and the square-root operator selectively enhances small peaks.

We start with the SNIP algorithm of the creation of baseline spectrum. In subsequent sections we shall generalize this algorithm for two, three and n-dimensional histograms.

2.1. *One dimensional spectrum*

Since the SNIP algorithm for one dimensional spectra is known [11, 12], we shall describe it only briefly. Let us suppose that we estimate baseline spectrum of one dimensional histogram stored in the vector $v(i)$, which was calculated from $y(i)$ according to (1). From $v(i)$ we shall calculate step by step the vectors $v_1(i), v_2(i)$ up to $v_m(i)$, where m is a given free parameter. The new value in the channel i in the p-th iteration step is obtained by comparison of average of the values $v_{p-1}(i-p), v_{p-1}(i+p)$ with the value $v_{p-1}(i)$. We accept the minimum of these values, i.e.,

$$v_p(i) = \min\ v_{p-1}(i), \frac{[v_{p-1}(i+p)\ +\ v_{p-1}(i-p)]}{2} \tag{2}$$

The situation within peak region is shown in Fig. 1.

Fig. 1

On the other hand an example of the situation outside of the peak region is illustrated in Fig. 2.

Fig. 2

After the vector $v_m(i)$ is calculated we have to apply the inverse LLS operator to obtain resulting baseline spectrum.

As a whole we can express the SNIP algorithm for one dimensional spectra in the form of C language commands. We shall start from the vector **v**. Moreover we need one working vector **w**, both of the length N. The number of required iterations m is supposed to be known.

Algorithm A

```
for (i=0; i<N; i++)
   v[i]=log(log(sqrt(y[i] + 1) +1) +1);        /*LLS operator*/
for (p=1; p<=m; p++){                          /*SNIP procedure*/
   for (i=p; i<N-p; i++){
            a1=v[i];
            a2=(v[i-p]+v[i+p])/2;
            w[i]=min(a1, a2);
   }
   for (i=p; i<N-p; i++)                       /*working vector*/
            v[i]=w[i];                         /*w is written back to v*/
}
for (i=0; i<N; i++)                            /*inverse LLS operator*/
   b[i]=exp(exp(v[i] -1) -1) * exp(exp(v[i] -1) -1) -1;
```

The resulting baseline spectrum is stored in the vector **b**. By its subtraction from the original vector **y** one gets pure peaks without background.

2.2. *Two dimensional spectrum*

Analogously to one dimensional background estimation one can proceed in derivation of an algorithm to determine background of two dimensional spectrum. Again in the first step, using operator (1), from the original spectrum $y(i,j)$ we compute matrix $v(i,j)$, $i \in < 0, N_1 - 1 >, j \in < 0, N_2 - 1 >$. From the two dimensional spectrum $v(i,j)$ we shall successively create matrices $v_1(i,j), v_2(i,j)$ up to $v_m(i,j)$.

To explain the algorithm of the calculation of a new value in the channel i,j, we shall employ Fig. 3. Let us imagine the situation that besides of linear background, also the crossing of two ridges occurs in the vicinity of the point i,j. One has to decide about presence of two-fold coincidence two dimensional peak at the point i,j.

Fig. 3

The matrix elements that enter background estimation in the p-th step are denoted

$$\begin{aligned} P_1 &= v_{p-1}(i+p,\ j+p); & P_2 &= v_{p-1}(i-p,\ j+p) \\ P_3 &= v_{p-1}(i+p,\ j-p); & P_4 &= v_{p-1}(i-p,\ j-p) \\ S_1 &= v_{p-1}(i+p,\ j); & S_2 &= v_{p-1}(i,\ j+p) \\ S_3 &= v_{p-1}(i,\ j-p); & S_4 &= v_{p-1}(i-p,\ j) \end{aligned} \tag{3}$$

Our aim is that the peak ridges in both directions (coincidences of peaks with linear background) as well as their sum were incorporated into the background estimate. Therefore we compare the values in the elements S with the average value of neighbouring elements P. Then we replace the new values S by the maximums, i.e.,

$$\begin{aligned} S_1 &= \max\{S_1,\ (P_1+P_3)/2\}; \\ S_2 &= \max\{S_2,\ (P_1+P_2)/2\}; \\ S_3 &= \max\{S_3,\ (P_3+P_4)/2\}; \\ S_4 &= \max\{S_4,\ (P_2+P_4)/2\}. \end{aligned} \tag{4}$$

Further we subtract the averages of neighbouring points P from appropriate points S. In this way we get the heights of peaks (without linear background) in the slices of the ridges.

$$\begin{aligned} S_1 &= S_1 - \ (P_1+P_3)/2; \\ S_2 &= S_2 - \ (P_1+P_2)/2; \\ S_3 &= S_3 - \ (P_3+P_4)/2; \\ S_4 &= S_4 - \ (P_2+P_4)/2. \end{aligned} \tag{5}$$

In the next step we calculate average values of opposite elements S and we add them to the average value of all elements P

$$a = (S_1+S_4)/2 + (S_2+S_3)/2 + (P_1+P_2+P_3+P_4)/4 \tag{6}$$

Then the new value in the matrix element i,j in the p-th iteration step is

$$v_p(i,j) = \min\{v_{p-1}(i,j),\ a\}. \tag{7}$$

Employing this algorithm one can include the linear background as well as both ridges in the vicinity of a peak into the created base-surface background spectrum. After subtracting the background spectrum from the original spectrum we get pure two dimensional coincidence peaks.

The procedure to calculate background spectrum of a two dimensional spectrum, expressed in C language commands, is as follows (we do not present LLS and inverse LLS operators at the beginning and at the end of the procedure, respectively):

Algorithm B

```
for (p=1; p<=m; p++){
    for (i=p; i<N1-p; i++){
        for (j=p; j<N2-p; i++){
            P1=v[i+p][j+p],    P2=v[i-p][j+p];
            P3=v[i+p][j-p],    P4=v[i-p][j-p];
            S1=v[i+p][j],    S2=v[i][j+p];
            S3=v[i][j-p],    S4=v[i-p][j];
            S1=max(S1,(P1+P3)/2)-(P1+P3)/2;
            S2=max(S2,(P1+P2)/2)-(P1+P2)/2;
            S3=max(S3,(P3+P4)/2)-(P3+P4)/2;
            S4=max(S4,(P2+P4)/2)-(P2+P4)/2;
            a1=v[i,j];
            a2=(S1+S4)/2+(S2+S3)/2+(P1+P2+P3+P4)/4;
            w[i][j]=min(a1, a2);
        }
    }
    for (i=p; i<N1-p; i++){
        for (j=p; j<N2-p; i++)
            v[i][j]=w[i][j];
    }
}
```

Let us illustrate the use of the above derived algorithm in a small example. Fig. 4 shows the sum of two one-fold Gaussians (ridges) generated by

$$50 \cdot \mathbf{e}^{\frac{-(x-64)^2}{20}} + 50 \cdot \mathbf{e}^{\frac{-(y-128)^2}{20}} \tag{8}$$

Fig. 4

Fig. 5 represents two-fold Gaussian

$$100 \cdot \mathbf{e}^{-[\frac{(x-64)^2}{20} + \frac{(y-128)^2}{20}]} \tag{9}$$

Fig. 5

and finally Fig. 6 is sum of Gaussians from Figs. 4 and 5.

Fig. 6

Based on visual assessment one can hardly predict the existence of the two-fold Gaussian positioned at the point of crossing of both ridges. When using our algorithm of two dimensional background elimination (m=18) we obtain two dimensional Gaussian that is exactly in correspondence with Fig.5.

Let us go ahead in these considerations. Let us slice the two fold two dimensional Gaussian from Fig.5. in the direction parallel with the y axis (x=64). We get one dimensional Gaussian given in Fig. 7.

Fig. 7

Then we make a slice of the sum of one and two-fold Gaussians given in Fig. 6, for x=64 too. This gives one dimensional Gaussian shown in Fig 8.

Fig. 8

Now applying one dimensional SNIP procedure ($m = 18$) to the data in the Fig. 8 yields one dimensional Gaussian shown in Fig. 9.

Fig. 9

However this result differs from the Gaussian given in Fig. 7. It contains the contribution of both two-fold Gaussian and one-fold Gaussian in y direction

$$50 \cdot \mathbf{e}^{\frac{-(y-128)^2}{20}} \tag{10}$$

False information is incorporated in the result. Naturally this is undesirable effect.

This implies, that the SNIP procedure must be applied in original space where the coincidence spectrum was measured and only after that one can make slices of the spectrum. If we first made slices and then applied appropriate SNIP procedure we would obtain also the contributions of lower-fold coincidences. Some peaks would be higher and also some new false peaks would appear.

2.3. *Three dimensional spectrum*

Here we shall suppose that we have three dimensional data array $v(i, j, k)$, $i \in< 0,\ N_1 - 1 >, j \in< 0,\ N_2 - 1 >, k \in< 0,\ N_3 - 1 >$, which was calculated from the three dimensional histogram $y(i, j, k)$ of the same lengths using (1). The situation, how the points entering the calculation of a new value in the channel i, j, k in the p-th iteration are positioned in three dimensional space, is shown in Fig. 10.

Fig. 10

To calculate a new value in each channel in each iteration step in one dimensional background estimation one needs 3 points, in two dimensional case 9 points and finally in three dimensional case 27 points.

In two dimensional case the ridges, i.e., coincidences peak-background in both directions $(p_1, b), (b, p_2)$, and implicitly their sum have been included into the created base-surface background spectrum. In three dimensional case one has to include the following combinations of coincidences

$$\begin{array}{lll} (p_1,\, b,\, b), & (b,\, p_2,\, b), & (b,\, b,\, p_3) \\ (p_1,\, p_2,\, b), & (p_1,\, b,\, p_3), & (b,\, p_2,\, p_3). \end{array} \tag{11}$$

i.e., one and two-fold coincidences peak-background, into the estimated base-volume background spectrum. The derivation of the algorithm of background estimation is analogous to that presented in the previous section. At the beginning we take outer edges of the cube shown in Fig. 10. We calculate new values S (they represent one-fold coincidences peak-background)

$$\begin{aligned}
S_1 &= \max\{S_1,\,(P_1+P_3)/2\} - (P_1+P_3)/2;\\
S_2 &= \max\{S_2,\,(P_1+P_2)/2\} - (P_1+P_2)/2;\\
S_3 &= \max\{S_3,\,(P_2+P_4)/2\} - (P_2+P_4)/2;\\
S_4 &= \max\{S_4,\,(P_3+P_4)/2\} - (P_3+P_4)/2;\\
S_5 &= \max\{S_5,\,(P_5+P_7)/2\} - (P_5+P_7)/2;\\
S_6 &= \max\{S_6,\,(P_5+P_6)/2\} - (P_5+P_6)/2;\\
S_7 &= \max\{S_7,\,(P_6+P_8)/2\} - (P_6+P_8)/2;\\
S_8 &= \max\{S_8,\,(P_7+P_8)/2\} - (P_7+P_8)/2;\\
S_9 &= \max\{S_9,\,(P_2+P_6)/2\} - (P_2+P_6)/2;\\
S_{10} &= \max\{S_{10},\,(P_4+P_8)/2\} - (P_4+P_8)/2;\\
S_{11} &= \max\{S_{11},\,(P_1+P_5)/2\} - (P_1+P_5)/2;\\
S_{12} &= \max\{S_{12},\,(P_3+P_7)/2\} - (P_3+P_7)/2.
\end{aligned} \tag{12}$$

Essentially the relations (12), which express one-fold coincidences peak-background, correspond to relations (4), (5). Also analogously to (6) we calculate new values R in the centers of sides of the cube

$$\begin{aligned}
R_1 &= \max\{R_1,(S_1+S_3)/2+(S_2+S_4)/2+(P_1+P_2+P_3+P_4)/4\};\\
R_2 &= \max\{R_2,(S_5+S_7)/2+(S_6+S_8)/2+(P_5+P_6+P_7+P_8)/4\};\\
R_3 &= \max\{R_3,(S_3+S_7)/2+(S_9+S_{10})/2+(P_2+P_4+P_6+P_8)/4\};\\
R_4 &= \max\{R_4,(S_1+S_5)/2+(S_{11}+S_{12})/2+(P_1+P_5+P_3+P_7)/4\};\\
R_5 &= \max\{R_5,(S_9+S_{11})/2+(S_2+S_6)/2+(P_1+P_2+P_5+P_6)/4\};\\
R_6 &= \max\{R_6,(S_4+S_8)/2+(S_{10}+S_{12})/2+(P_3+P_4+P_7+P_8)/4\}.
\end{aligned} \tag{13}$$

From these values we subtract average values of one-fold coincidences peak-background in both directions as well as the average value of linear background (points P) on each side of the cube

$$\begin{aligned}
R_1 &= R_1-[(S_1+S_3)/2+(S_2+S_4)/2+(P_1+P_2+P_3+P_4)/4];\\
R_2 &= R_2-[(S_5+S_7)/2+(S_6+S_8)/2+(P_5+P_6+P_7+P_8)/4];\\
R_3 &= R_3-[(S_3+S_7)/2+(S_9+S_{10})/2+(P_2+P_4+P_6+P_8)/4];\\
R_4 &= R_4-(S_1+S_5)/2+(S_{11}+S_{12})/2+(P_1+P_5+P_3+P_7)/4];\\
R_5 &= R_5-(S_9+S_{11})/2+(S_2+S_6)/2+(P_1+P_2+P_5+P_6)/4];\\
R_6 &= R_6-(S_4+S_8)/2+(S_{10}+S_{12})/2+(P_3+P_4+P_7+P_8)/4].
\end{aligned} \tag{14}$$

Further we compute the average value of the contribution of all points P, all edges S and all sides R with appropriate weights

$$
\begin{aligned}
a \;=\; & (R_1 + R_2)/2 + (R_3 + R_4)/2 + (R_5 + R_6)/2 + \\
& + (S_1 + S_3 + S_5 + S_7)/4 + \\
& + (S_2 + S_4 + S_6 + S_8)/4 + \\
& + (S_9 + S_{10} + S_{11} + S_{12})/4 + \\
& + (P_1 + P_2 + P_3 + P_4 + P_5 + P_6 + P_7 + P_8)/8.
\end{aligned} \tag{15}
$$

Then the new value in the point i, j, k in p-th iteration is

$$v_p(i,j,k) = \min\{v_{p-1}(i,j,k),\, a\}. \tag{16}$$

Employing this algorithm one can estimate three dimensional base-volume background spectrum including linear background as well as one and two-fold coincidences peak-background. After subtracting it from the original spectrum one gets pure three-fold three dimensional peaks. The procedure SNIP to create three dimensional background spectrum is obvious from two previous cases.

For the sake of illustration we present a small example. To make things about dimensionality clearer in Fig 11 we give an example of the sum of three one-fold coincidences of peak-background in three dimensional space

$$20 \cdot \mathbf{e}^{\frac{-(x-16)^2}{2}} + 20 \cdot \mathbf{e}^{\frac{-(y-16)^2}{2}} + 20 \cdot \mathbf{e}^{\frac{-(z-16)^2}{2}}. \tag{17}$$

Fig. 11

In Fig. 12 we present the sum of two-fold coincidences Gaussian-background in three dimensional space

$$20 \cdot \mathbf{e}^{-\left[\frac{(x-16)^2}{2} + \frac{(y-16)^2}{2}\right]} + 20 \cdot \mathbf{e}^{-\left[\frac{(x-16)^2}{2} + \frac{(z-16)^2}{2}\right]} + 20 \cdot \mathbf{e}^{-\left[\frac{(y-16)^2}{2} + \frac{(z-16)^2}{2}\right]}. \tag{18}$$

and in Fig. 13 three-fold Gaussian

$$60 \cdot \mathbf{e}^{-\left[\frac{(x-16)^2}{2} + \frac{(y-16)^2}{2} + \frac{(z-16)^2}{2}\right]} \tag{19}$$

Fig. 12, 13

Finally in Fig. 14 one can see the sum of all Gaussians according to (17), (18), (19).

Fig. 14

Apparently nobody can say anything about the existence of three-fold Gaussian, which is of particular interest. However when applying above derived algorithm (12), (13), (14), (15), (16) ($m = 5$) we get three dimensional Gaussian, which is exactly the same as the original one presented in Fig. 13.

If we want to create one or two dimensional slices from a three dimensional spectrum first we have (as mentioned in the previous section) to estimate and subtract background in three dimensional space using three dimensional SNIP algorithm. Then we can make slices. Otherwise in the slices we get false information.

2.4. n – ***dimensional spectrum***

On the grounds mentioned above it can be of interest to view how the background estimation algorithm can be generalized for n-dimensional spectra. In what follows we outline briefly the derivation of such an algorithm. For the sake of better understanding, along the derivation, we shall give instances for 4-dimensional spectrum.

To correct one point in p-th iteration step in n-dimensional spectrum $v_p(i_0, i_1, \ldots, i_{n-1})$ 3^n points $v_{p-1}(x_0, x_1, \ldots, x_{n-1})$, where $x_j = i_j + p, i_j, i_j - p$; $j = 0, 1, ldots, n-1$, enter the calculation (3, 9, or 27 points in one, two or three dimensional case, respectively). To simplify the notation we shall denote the position coordinates of the points v_{p-1} only by signs $+, 0, -$. For example in 4-dimensional background estimation the points entering the correction of one point are

$$\begin{array}{l} v_{p-1}(+,\quad +,\quad +,\quad +) \\ v_{p-1}(+,\quad +,\quad +,\quad 0\,) \\ v_{p-1}(+,\quad +,\quad +,\quad -) \\ v_{p-1}(+,\quad +,\quad 0,\quad +) \\ v_{p-1}(+,\quad +,\quad 0,\quad 0\,) \\ \qquad\qquad\vdots \\ v_{p-1}(-,\quad -,\quad -,\quad 0\,) \\ v_{p-1}(-,\quad -,\quad -,\quad -)\,. \end{array} \tag{20}$$

We divide the points v_{p-1} of n-dimensional space into $n+1$ classes according to number of zeros in the position coordinates

$$^0v_{p-1},\ ^1v_{p-}1, ...,\ ^{n-1}v_{p-1},\ ^nv_{p-1}, \tag{21}$$

We denoted the class by the left upper index. The class 0 contains 2^n points, the class 1 $\begin{pmatrix} n \\ 1 \end{pmatrix} 2^{n-1}$ points, the class k $\begin{pmatrix} n \\ k \end{pmatrix} 2^{n-k}$ points and class n contains 1 point. Successively we can carry out the correction in the points of the class 1 (it is entered by points of the class 0), then in the points of the class 2 (it is entered by points of classes 0, 1), generally in the points of the class k (it is entered by points of classes $0, 1, ..., k-1$) up to the class n. In the previous section we denoted the points of the class 0 by P, points of the class 1 by S and the class 2 by R. For instance in 4-dimensional case the coordinates of points of the class 1 are given in the Table 1.

Table 1.

The correction of one point in the class 1 resides in finding its neighbours in the class 0, calculation of the maximum of this point by its comparison with the average value of the neighbours and subtraction of the average value of the neighbours (see (4), (12). The neighbours of a given point can be simply found by replacing of the coordinate 0 by $+,-$. As an example for $n=4$ we carry out the correction of the point

$$\begin{aligned} {}^1v_{p-1}(+,0,+,-) \;&=\; \max\Big\{{}^1v_{p-1}(+,0,+,-), \\ &\qquad \Big({}^0v_{p-1}(+,+,+,-) + {}^0v_{p-1}(+,-,+,-)\Big)/2\Big\} - \\ &\quad - \Big({}^0v_{p-1}(+,+,+,-) + {}^0v_{p-1}(+,-,+,-)\Big)/2 \end{aligned} \tag{22}$$

After the correction of all points of the class 1 is finished we carry out the correction of points of the class 2. For n=4, in the Table 2, we give coordinates of all points of the class 2.

Table 2.

For the correction of a point in the class 2 we need neighbours of the classes 1 and 0. We can find the neighbours of the class 1 by replacing the first coordinate 0 by the coordinates $+,-$ and then the second coordinate 0 by the coordinates $+,-$. The neighbours of the class 0 can be found by replacing of both coordinates 0 by all combinations of the coordinates $+,-$. For example for $n=4$ the point of the class 2

$$(+,\,0,\,-,\,0)$$

has the neighbours of the class 1

$$(+,\,0,\,-,\,+),\;\;(+,\,0,\,-,\,-)$$

and the neighbours of the class 0

$$(+,\,+,\,-,\,+),\;\;(+,\,+,\,-,\,-),\;\;(+,\,-,\,-,\,+),\;\;(+,\,-,\,-,\,-).$$

Hence in the correction in the point ${}^2v_{p-1}(+,0,-,0)$ we calculate

$$\begin{aligned} a \;=\; &\Big({}^1v_{p-1}(+,0,-,+) + {}^1v_{p-1}(+,0,-,-) + \\ &\qquad + {}^1v_{p-1}(+,+,-,0) + {}^1v_{p-1}(+,-,-,0)\Big)\cdot\frac{1}{2} + \\ &+ \Big({}^0v_{p-1}(+,+,-,+) + {}^0v_{p-1}(+,+,-,-) + \\ &\qquad + {}^0v_{p-1}(+,-,-,+) + {}^0v_{p-1}(+,-,-,-)\Big)\cdot\frac{1}{4} \end{aligned} \tag{23}$$

and

$${}^2v_{p-1}(+,0,-,0) = \max\{{}^2v_{p-1}(+,0,-,0),\,a\} - a. \tag{24}$$

In general in the correction of a point of the class k we have to sum all neighbours of the class $k-1$ divided by 2, then to add all neighbours of the class $k-2$ divided by 4, ..., to add all neighbours of the class $k-r$ divided by 2^{k-r}, and so on, up to all neighbours of the class 0 divided by 2^k. After summing up all neighbours in this way we proceed analogously to (15). We assumed that the neighbours have been determined using the above given algorithm. The point in the class k has $2^{k-r}\begin{pmatrix} k \\ r \end{pmatrix}$ neighbours of the class r. Provided that a point of the class k has zeros in the coordinates $t_1, t_2, \ldots, t_k$ one obtains

$$a = \sum_{r=o}^{k-1} \left(\sum {}^r v_{p-1}(x_0, x_1, \cdots x_n) \right) \cdot \frac{1}{2^{k-r}} \tag{25}$$

where the inner sum is carried out over $2^{k-r} \begin{pmatrix} k \\ r \end{pmatrix}$ combinations of $+, -$ in coordinates $t_1, t_2, \ldots, t_k$.

For $k = 1, 2, \ldots, n-1$ we carry out the correction

$${}^k v_{p-1}(x_0, x_1, \ldots, x_n) = \max\{{}^k v_{p-1}(x_0, x_1, \ldots, x_n),\, a\} - a. \tag{26}$$

Finally for $k = n$ we calculate

$${}^k v_p(i_0, i_1, \ldots, i_n) = \min\{{}^k v_{p-1}(i_0, i_1, \ldots, i_n),\, a\}, \tag{27}$$

which represents the resulting corrected value of the point in the p-th iteration. By correcting all values of n-dimensional histogram and repeating the whole procedure m-times we obtain the background spectrum, which contains linear background, one-fold, two-fold, up to $n-1$-fold coincidences peak-background. After subtracting the background spectrum from the original n-dimensional spectrum one gets n-dimensional spectrum of n-fold coincidences.

3. Experimental results

The algorithms of background estimation derived in the previous chapter have been implemented in the multiparameter nuclear data acquisition and processing system [13]. They have been employed to process one, two and three dimensional spectra from experiments in LBNL Berkeley, which are realized in collaboration with Vanderbilt University, JINR Dubna, Idaho National Engineering Laboratory and Oak Ridge National Laboratory.

An example of one dimensional spectrum before and after subtraction the background estimated by the described method ($m = 6$) is shown in Figs. 15,16.

Fig 15,16

Next we shall study the influence of the parameter m on the calculated background and mainly on the peak areas after background subtraction. The investigated peaks are drawn in Figs 15, 16 by thick line. We shall use two parameters, peak total counts - PTC and peak net counts - PNC (after subtraction of linear background in the peak region). Now let us define the coefficient of peak net counts preservation

$$r(m) = \frac{\mathrm{PNC}(m)}{\mathrm{PNC}_o} \cdot 100[\%] \tag{28}$$

where PNC(m) is PNC of the peak after subtraction of background estimated with parameter m and PNC_o is PNC of the peak in original spectrum. Further let us define the coefficient of background elimination efficiency

$$t(m) = \frac{\mathrm{PNC}(m)}{\mathrm{PTC}(m)} \cdot 100[\%] \tag{29}$$

We have evaluated both peaks for $m \in < 1, 20 >$. The results are presented in Figs 17, 18 ($r(m)$ - solid line, $t(m)$ - dashed line).

Fig 17,18

Obviously for $m \geq 6$ the net peak areas remain preserved. Moreover for $m = 6$ the net peak area is almost identical with the total peak area, i.e., the background is completely removed ($t(6) \approx 100\%$). To propose a suitable m parameter one can use

$$2m + 1 = w \tag{30}$$

where w is real width of an object (peak, doublet, multiplet) that should be preserved. Choosing too big m accounts for remaining background residua under peaks. We desire to remove the background under peaks to the highest possible extent as well as to preserve the net peak areas. The influence of the m parameter on the form of estimated background is illustrated in Fig. 19.

Fig. 19

Furthermore we have tested the algorithm of background elimination for two dimensional spectra. An example of two dimensional $\gamma - \gamma$ ray spectrum is given in Fig. 20. The spectrum contains relatively low level of background with small number of big peaks.

Fig. 20

The result after background elimination ($m = 8$), using the algorithm derived in the chapter 2, is shown in Fig. 21.

Fig. 21

In Fig. 22 we give an example of two dimensional spectrum with higher level of background and ridges and considerable number of narrow peaks. The spectrum is presented in the display mode "contours".

Fig. 22

Again after background elimination ($m = 8$) we obtained the result shown in Fig. 23.

Fig. 23

The last example in Fig. 24 presents $\gamma - X$-ray spectrum with asymmetrical lower and wider peaks and with higher level of background.

Fig. 24

The result after background elimination ($m = 20$) is shown in Fig. 25.

Fig. 25

Finally in Fig 26 we introduce an example of the original three dimensional spectrum. The cube (64x64x64 channels) was cut out of the data cube of $\gamma - \gamma - \gamma$-ray coincidences from GAMMASPHERE [1]. The original data with 4096 channels in each dimension were compressed to 904 channels. Utilizing the knowledge about the symmetry of the cube permitted the creation of tetrahedron with data volume reduced 6 times to the 252 MB. An alternative way of nuclear data compression is dealt with in [14].

Fig. 26

After applying the algorithm of background elimination for three dimensional spectra ($m = 5$) we get pure three-fold coincidence peaks in Fig. 27.

Fig. 27

In Figs. 28 and 29 we present the same spectra from Figs 26 and 27, respectively, in isosurface display mode. The isosurface divides the three dimensional space to two subspaces. The inner subspace contains the events with higher counts than a given value (in our case 100) and the outer subspace contains the events with lower counts.

Fig. 28,29

In Fig. 29 one can observe that the subspaces of the peaks of three-fold coincidences are well separated from the background and from one and two-fold coincidences peak-background represented by ridges.

Practical meaning of background elimination in original two dimensional space together with experimental results, are given in the next example. When Ge detectors in multidetector spectrometers to measure the γ-ray spectra that follow a fission and H.I. reaction involving neutrons are used many of spurios peaks can appear. Well known intensive peaks are seen in the γ-ray spectra due to inelastic neutron scattering of the first excited states of the germanium isotopes in the detector. For example such peaks are shown in region around 600keV (Fig. 30.) produced by $(n, n'\gamma)$ reaction on Ge isotopes. Broad saw-tooth lines result from production of charge in diode structure by the recoiling of Ge atoms produced in the inelastic scattering events. Because of their uncorrelated character relatively to the coincidence spectra efficency of the derived method of the background elimination can be seen by comparison of Fig. 30b and 30c. Apperently in Fig. 30c the false peak, which origin from the crossing ridges dissapeared.

Fig. 30

4. Conclusions

In the paper we have derived the algorithms of background elimination for two and three dimensional nuclear spectra. As one can see from the presented subroutines in C language the algorithms are simple and their implementation is realizable also on PC computers.

The algorithm of background elimination was generalized also for n-dimensional spectra. Its implementation for 4 and more dimensional spectra is, in principle, just matter of combinations.

Using the examples of synthetic (generated) data in the chapter 2 we have shown that the procedures of background elimination gave exactly expected results. The application of the algorithms for experimental data has been demonstrated in the chapter 3. We have studied also the influence of m parameter on the net peak areas.

In the algorithms presented we have changed the m parameter from 1 to a given chosen value. In two and three dimensional spectra we have changed the m parameter for each dimension in the same manner. The strategy how to drive m parameter during background estimation (the initial value of m, its increment, the selection of different m parameters for different dimensions) are subject of research in future.

The extension of the background elimination algorithm for the second and third dimension allowed to remove false peaks, which arise at the crossing points of ridges as their sum. Likewise it allowed to remove false peaks in one dimensional slices across the ridges.

After the preprocessing presented in the paper the peaks can be easily identified, fitted etc. To unfold pure background-free doublets and multiplets one can employ deconvolution methods described in [15], [16].

All three algorithms of background elimination in one, two and three dimensional spectra, respectively, are implemented in "Integrated Multiparameter Nuclear Data Analysis Package" [16].

Acknowledgements

The work is supported in part by the Grant Agency of Slovak Republic through contract GAV 2/1155/94. The authors would like to thanks the GAMMASPHERE collaboration, to J. H. Hamilton, J. O. Rasmussen, G. M. Ter-Akopian and A. V. Daniel, for help in data preperation and valuable discussions.

References

1. GAMMASPHERE a National Gamma-Ray Facility, a proposal, March 1988, Ed.: M. A. Delaplanque and R. M. Diamond.
2. F. A. Beck, Prog. Part. Nucl. Phys., 28 (1992) 443.
3. C. Rossi-Alvarez, Nucl. Phys. News Europe, 3 (1993) 10.
4. G. Palameta and J. C. Waddington, Nucl. Instr. and Meth, A234 (1985) 476.
5. S. Flibotte et al., Nucl. Instr. and Meth. A320 (1992) 325.
6. M. G. Chemaly and H. C. Griffin, Nucl. Instr. and Meth. A353 (1994) 296.
7. B. Crowell et al., Nucl. Instr. and Meth. A355 (1992) 572.
8. A. G. Smith and W. J. Vermeer, Nucl. Instr. and Meth. A350 (1994) 314.
9. D. C. Radford, Nucl. Instr. and Meth. A361 (1995) 297.
10. D. C. Radford, Nucl. Instr. and Meth. A361 (1995) 306.
11. C. G. Ryan, E. Clayton, W. L. Griffin, S. H. Sie and D. R. Cousens, Nucl. Instr. and Meth. B34 (1988) 396.
12. C. V. Hampton, B. Lian, Wm. C. Harris, Nucl. Instr. and Meth. A353 (1994) 280.
13. Morhac M., Turzo I., Kristiak J., IEEE Trans. on Nucl. Sci. 42 (1995) 1.
14. M. Morhac, V. Matousek, Nucl. Instr. and Meth. A370 (1996) 499.
15. P. Bandzuch, M. Morhac, J. Kristiak, Nucl. Instr. and Meth. A384 (1997) 506.
16. M. Morhac, J. Kliman, V. Matousek, I. Turzo, Integrated multiparameter nuclear data analysis package. Nucl. Instr. and Meth. Section A (1997) In press.

Figure captions

1. Illustration of SNIP algorithm for peak region of the spectrum.
2. Illustration of SNIP algorithm outside of peak region.
3. Situation for two dimensional background estimation in region of ridges crossing.
4. The sum of two one-fold Gaussians in two dimensional space.
5. Two-fold Gaussian in two dimensional space.
6. The sum of one-fold and two-fold two dimensional Gaussians from Figs. 4, 5.
7. One dimensional Gaussian obtained as a slice of the spectrum from Fig. 5 for $x = 64$.
8. One dimensional Gaussian plus background as a slice of the spectrum from Fig. 6 for $x = 64$.
9. One dimensional Gaussian obtained from the spectrum shown in Fig. 8 using one dimensional SNIP procedure for $m = 18$.
10. Points entering one iteration step in three dimensional background estimation.
11. The sum of three one-fold Gaussians in three dimensional space. The channels are presented as spheres. Their diameters are proportional to the counts in channels.
12. The sum of three two-fold Gaussians in three dimensional space.
13. Three-fold Gaussian in three dimensional space.
14. The sum of all one, two and three-fold Gaussians from Figs. 11, 12,13.
15. Original one dimensional experimental spectrum.
16. One dimensional spectrum from Fig. 15 after background estimation ($m = 6$) and subtraction.
17. Dependence of the coefficient of peak net counts preservation (solid line) and background elimination efficiency (dashed line) on m parameter for the peak 1.
18. Dependence of the coefficient of peak net counts preservation (solid line) and background elimination efficiency (dashed line) on m parameter for the peak 2.
19. Illustration of the influence of m parameter ($m = 4, 6, 14$) on the estimated background shape.
20. An example of $\gamma - \gamma$ ray spectrum (256x256 channels).
21. Spectrum from Fig. 20 after background elimination with $m = 8$.
22. An example of $\gamma - \gamma$ ray spectrum (256x256 channels).
23. Spectrum from Fig. 22 after background elimination with $m = 8$.
24. An example of $\gamma - X$-ray spectrum (256x256 channels) with asymmetrical peaks.

25. Spectrum from Fig. 24 after background elimination with $m = 20$.
26. An example of $\gamma - \gamma - \gamma$ ray spectrum (64x64x64 channels). Channels are shown as spheres with diameter proportional to counts they contain.
27. Three dimensional spectrum from Fig. 26 after background elimination with $m = 5$.
28. Three dimensional spectrum from Fig. 26 shown in isosurface display mode.
29. Three dimensional spectrum from Fig. 28 after background elimination ($m = 5$) shown in isosurface display mode.
30. Coincidence spectra from single gated two-fold data showing transitions in ^{104}Xe and Ru isotopes accompanying fission fragment pairs (a) without background elimination, (b) after one dimensional background elimination from (a) and (c) after two dimensional background elimination in two-fold $\gamma - \gamma$ coincidence matrix.

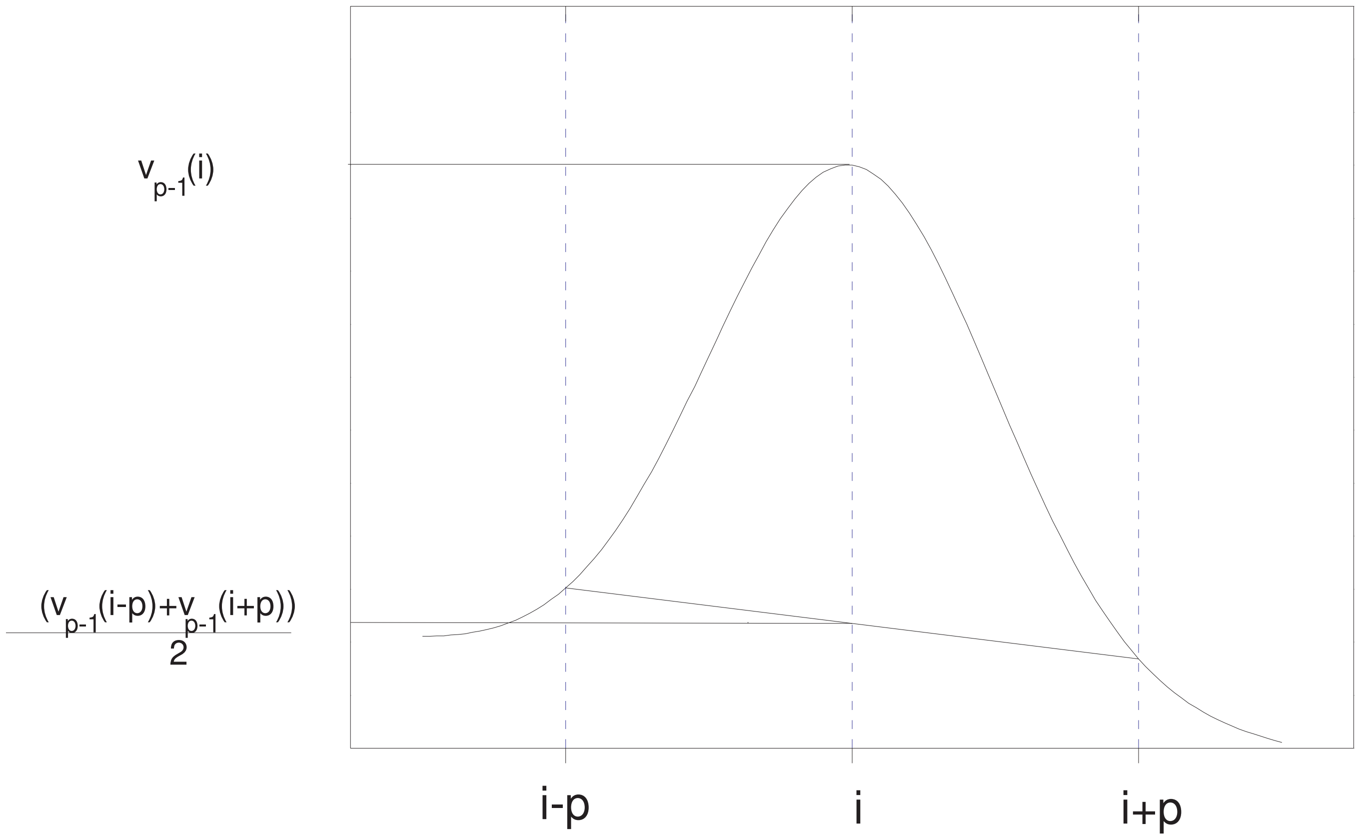

Fig.1 Illustration of SNIP algorithm for peak region of the spectrum.

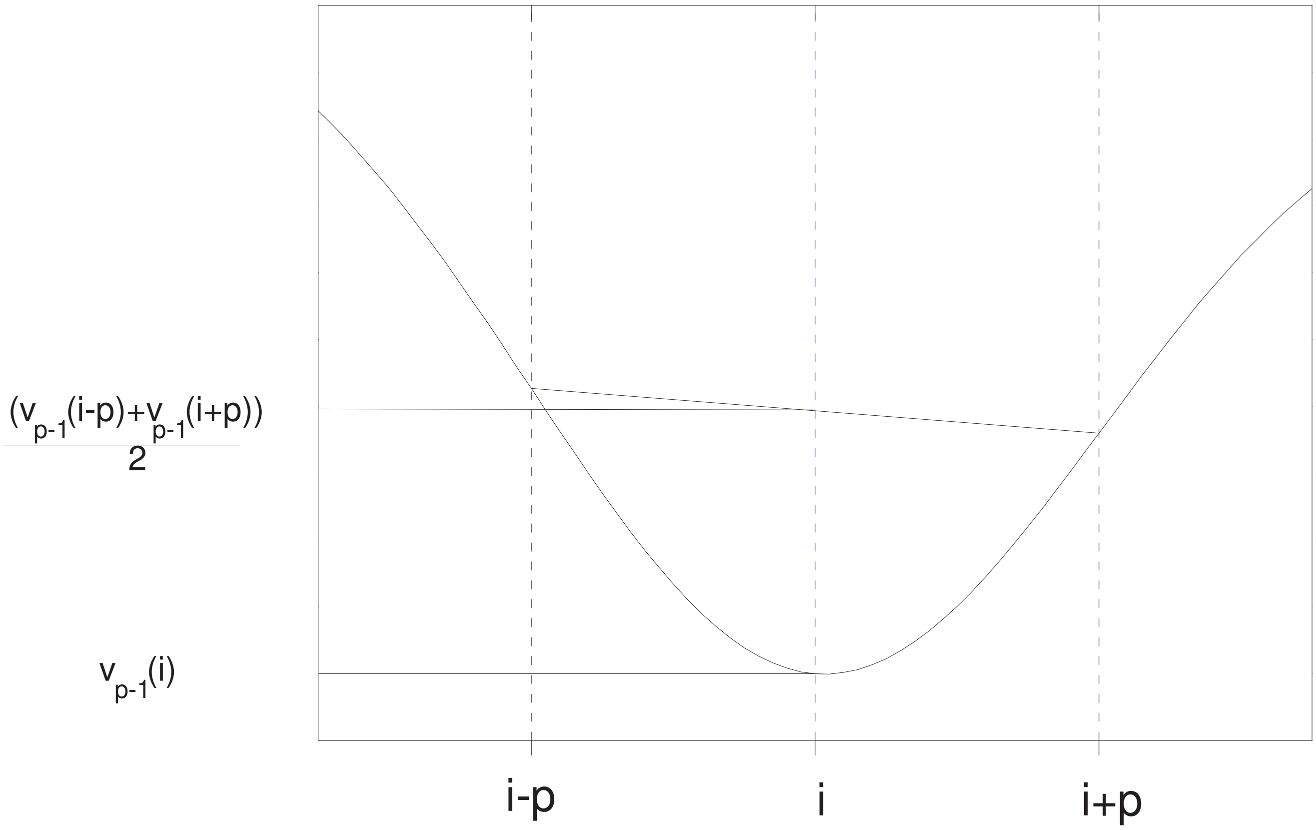

Fig.2 Illustration of SNIP algorithm outside of peak region.

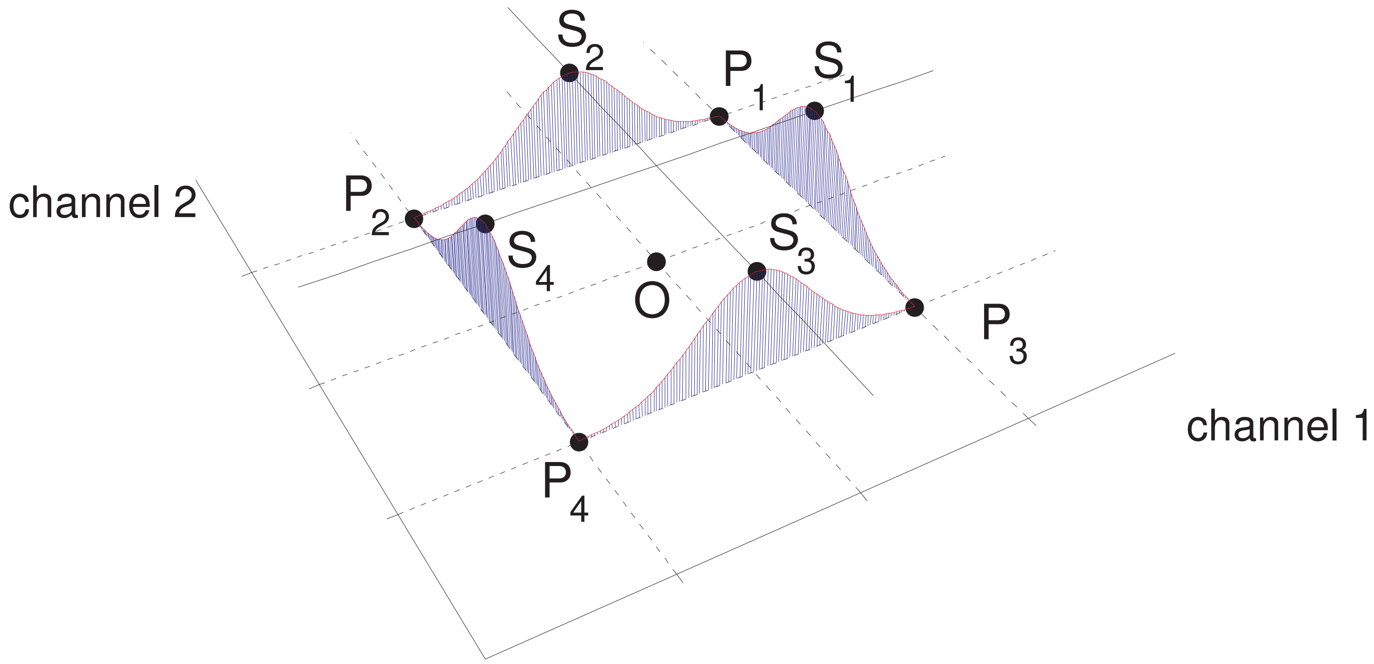

Fig.3 Situation for two dimensional background estimation in region of ridges crossing.

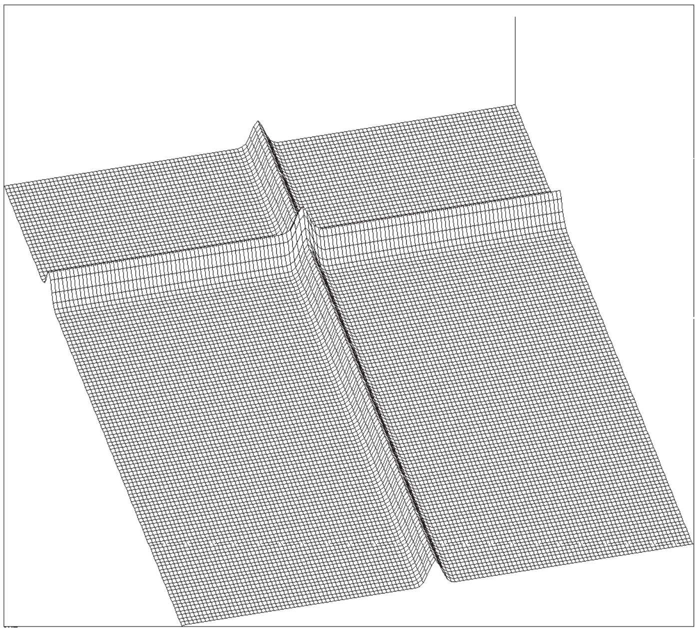

Fig.4 The sum of two one-fold Gaussians in two dimensional space.

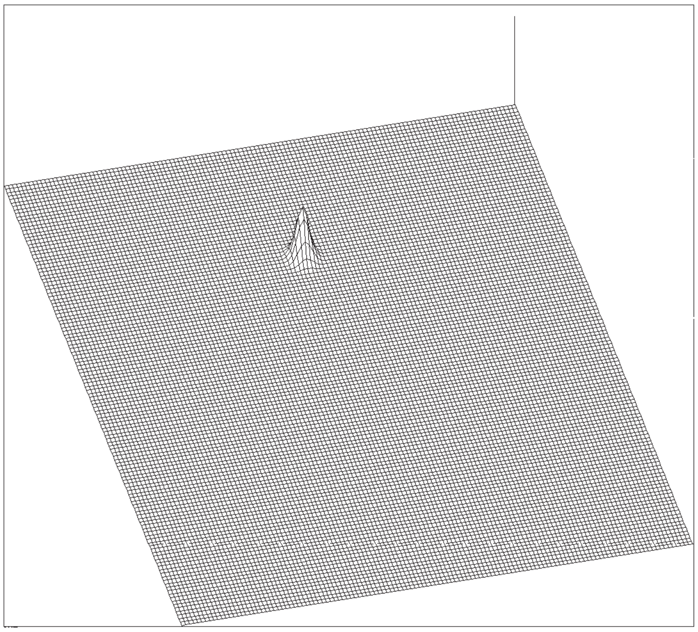

Fig.5 Two-fold Gaussian in two dimensional space.

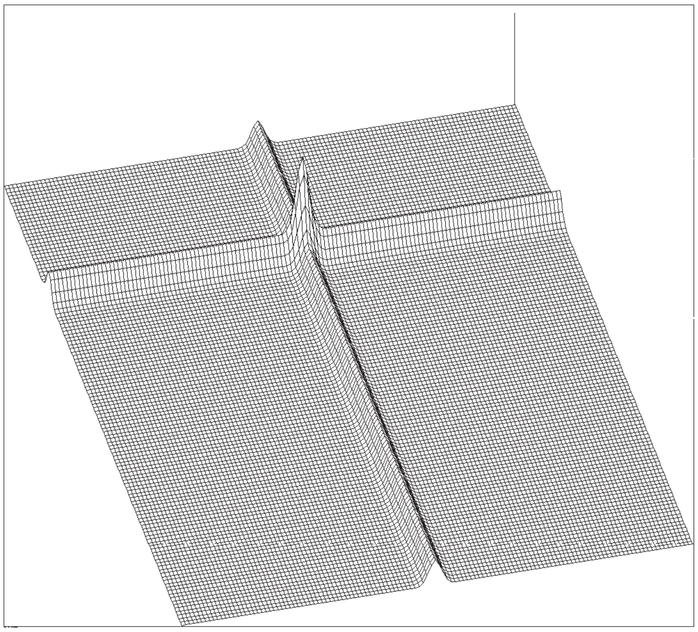

Fig.6 The sum of one-fold and two-fold two dimensional Gaussians from Figs. 4, 5.

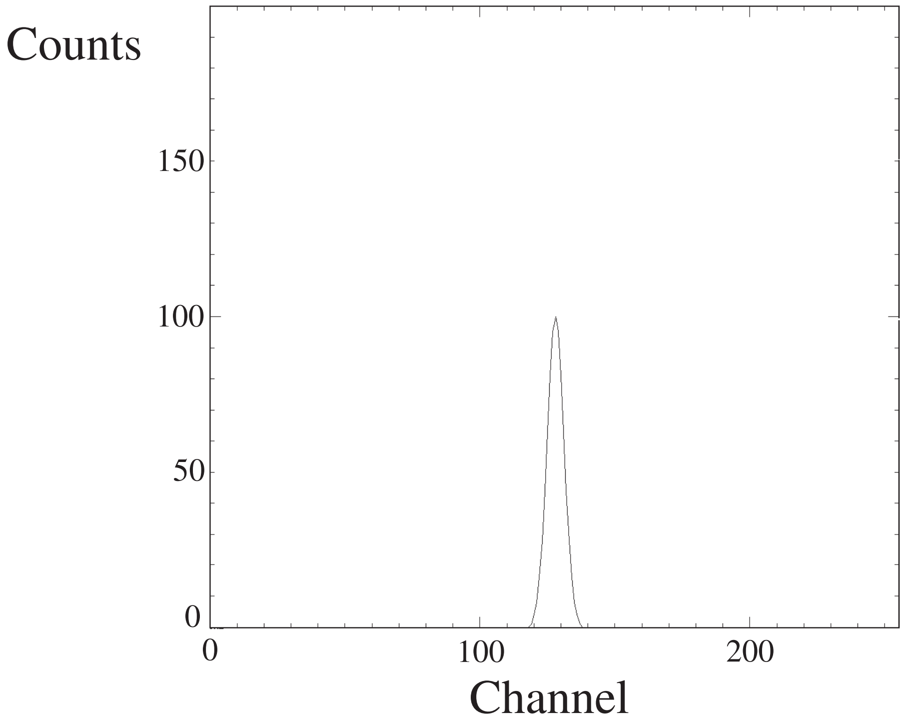

Fig.7 One dimensional Gaussian obtained as a slice of the spectrum from Fig. 5 for $x = 64$.

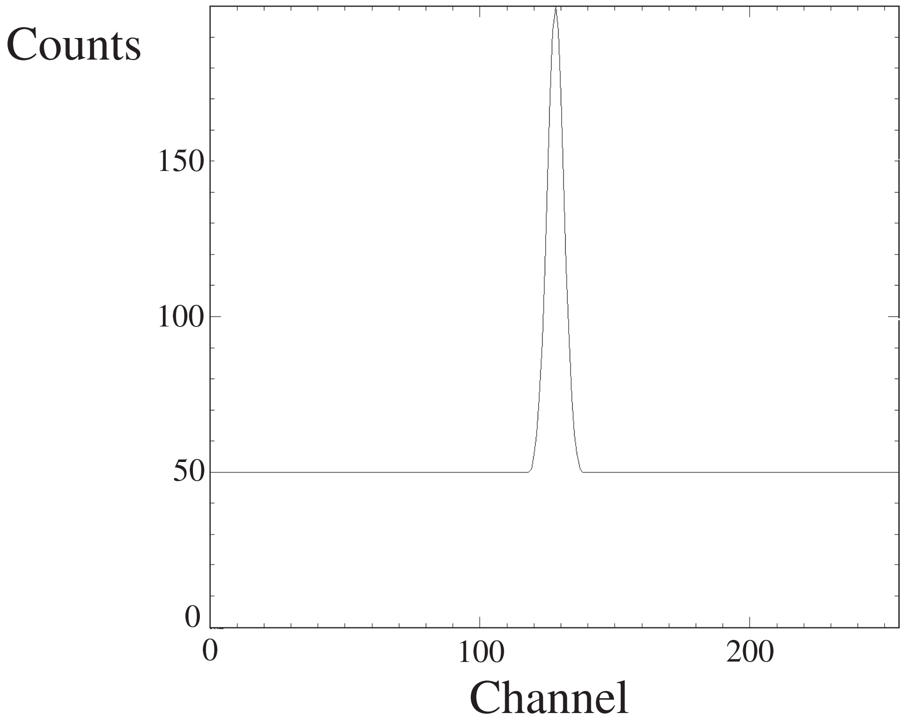

Fig.8 One dimensional Gaussian plus background as a slice of the spectrum from Fig. 6 for $x = 64$.

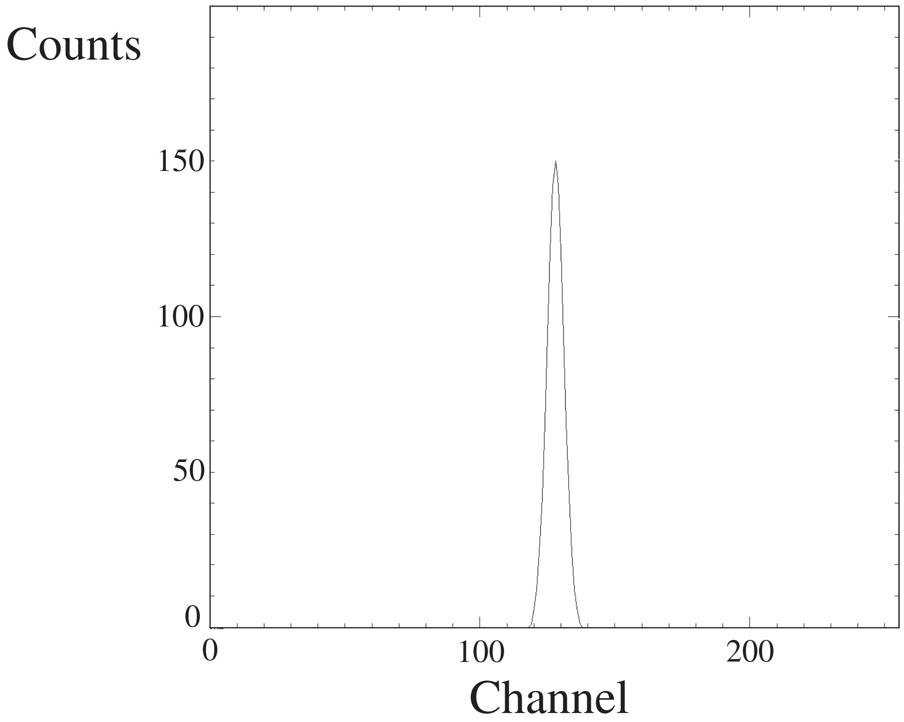

Fig.9 One dimensional Gaussian obtained from the spectrum shown in Fig. 8 using one dimensional SNIP procedure for $m = 18$.

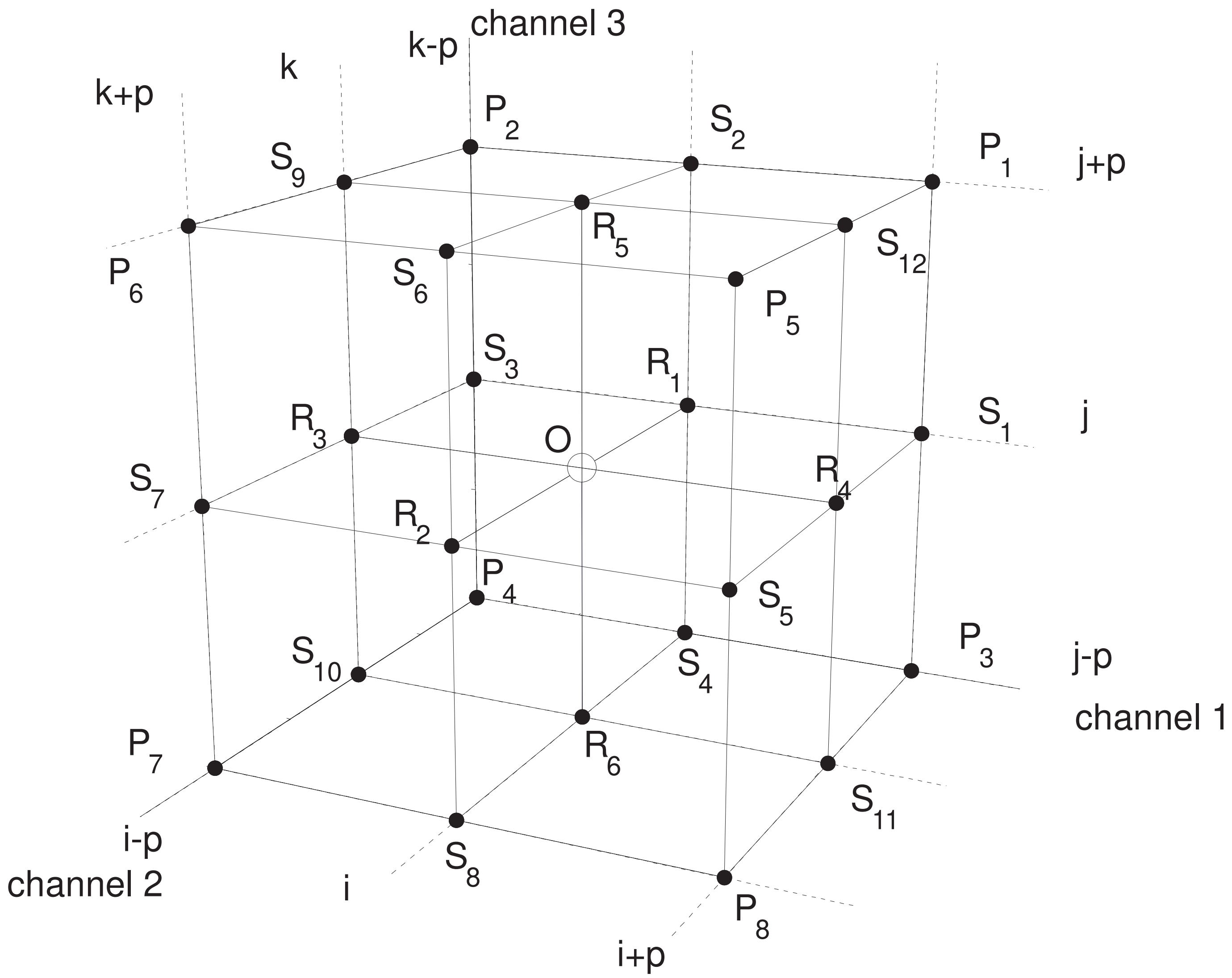

Fig.10 Points entering one iteration step in three dimensional background estimation.

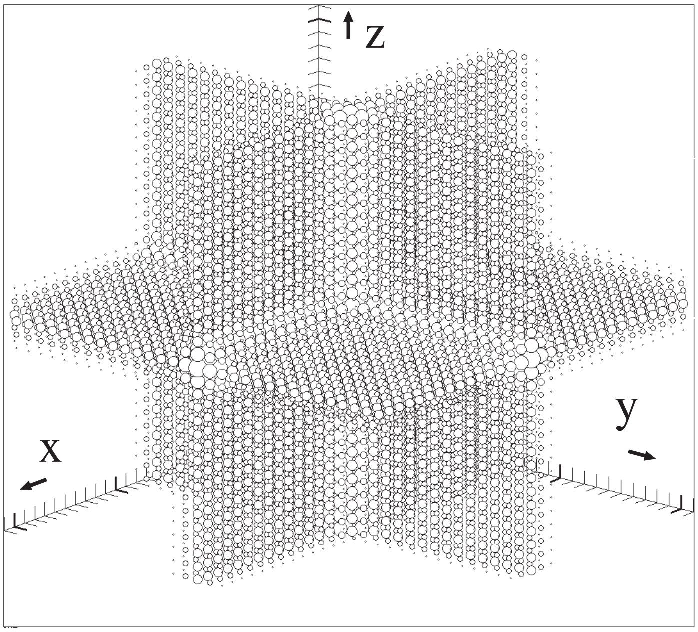

Fig.11 The sum of three one-fold Gaussians in three dimensional space. The channels are presented as spheres. Their diameters are proportional to the counts in channels.

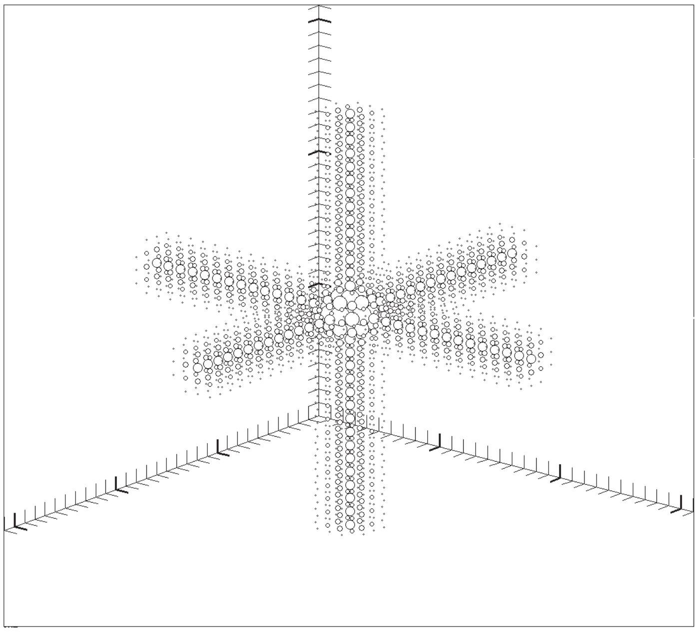

Fig.12 The sum of three two-fold Gaussians in three dimensional space.

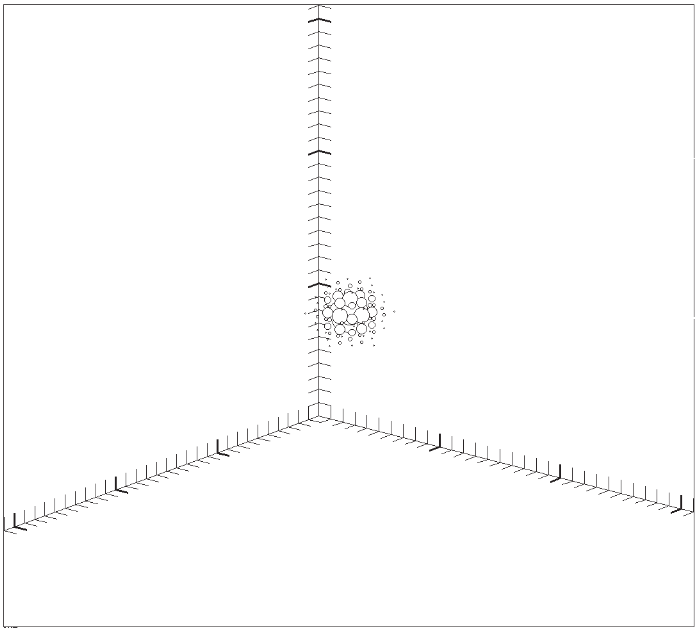

Fig.13 Three-fold Gaussian in three dimensional space.

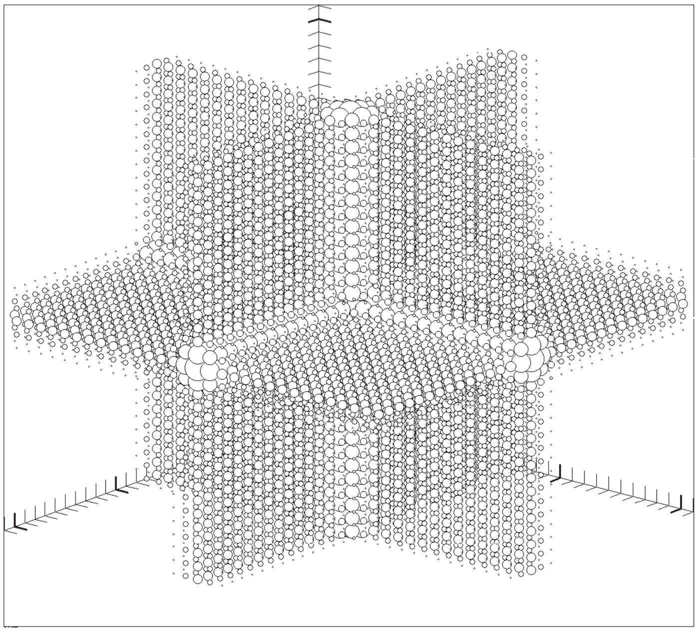

Fig.14 The sum of all one, two and three-fold Gaussians from Figs. 11, 12,13.

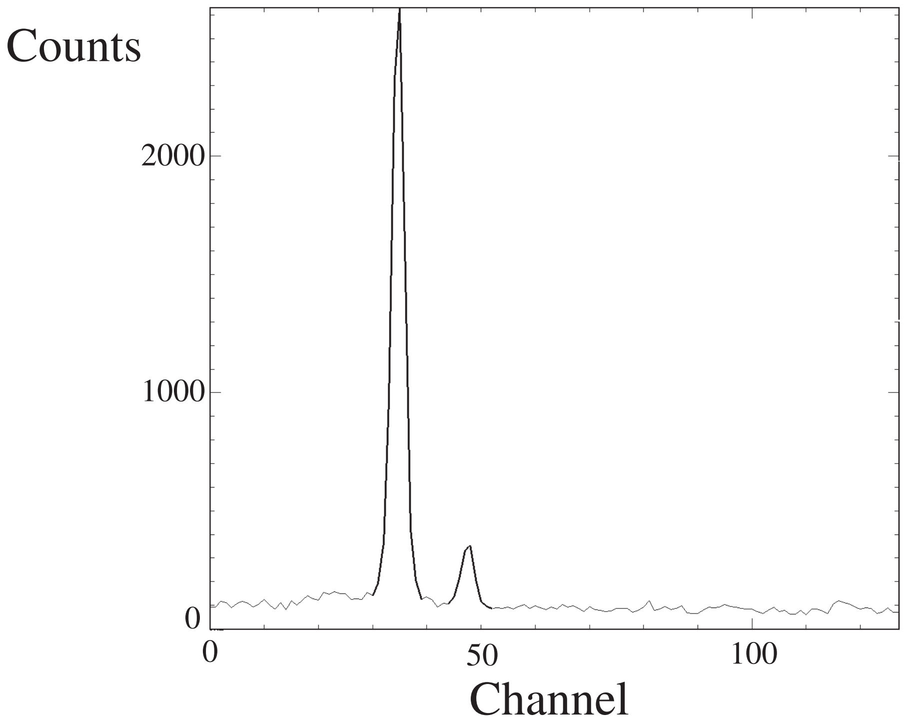

Fig.15 Original one dimensional experimental spectrum.

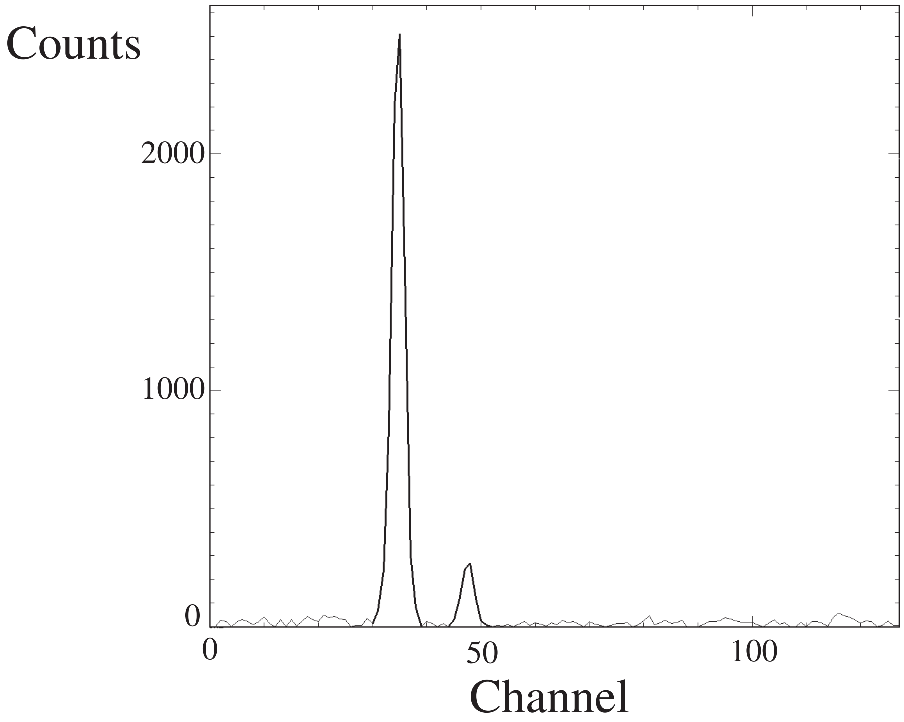

Fig.16 One dimensional spectrum from Fig. 15 after background estimation ($m = 6$) and subtraction.

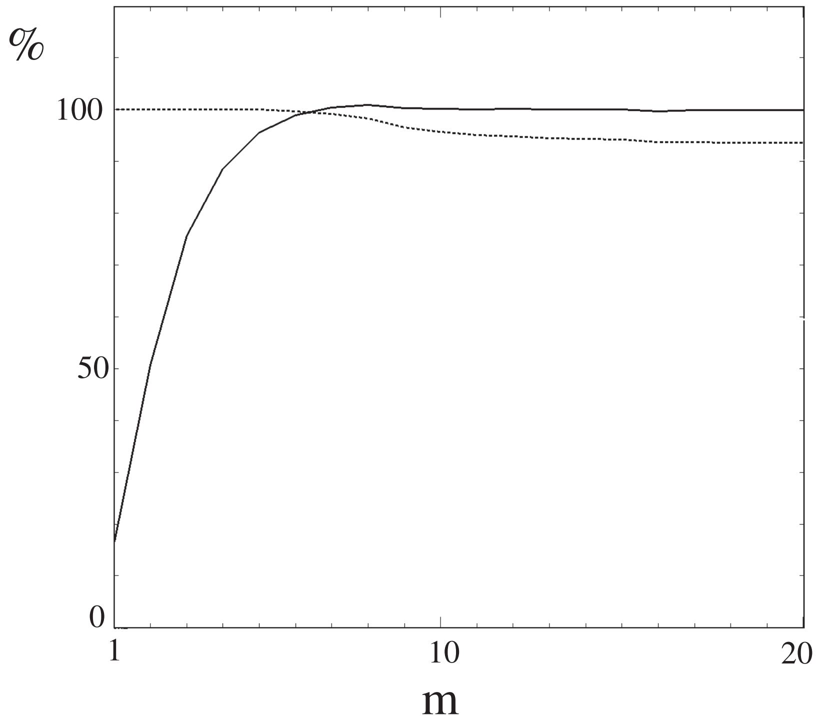

Fig.17 Dependence of the coefficient of peak net counts preservation (solid line) and background elimination efficiency (dashed line) on m parameter for the peak 1.

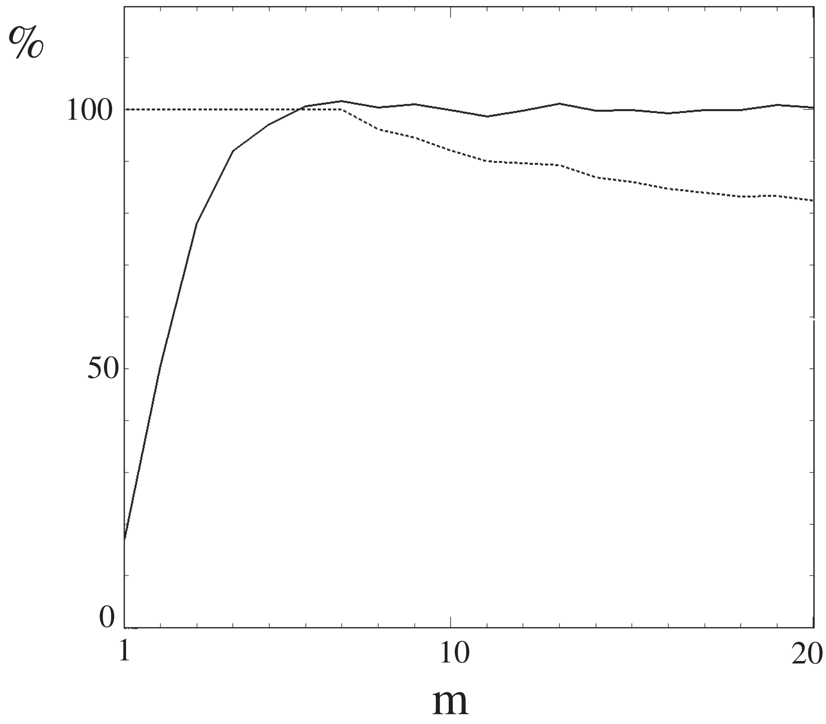

Fig.18 Dependence of the coefficient of peak net counts preservation (solid line) and background elimination efficiency (dashed line) on m parameter for the peak 2.

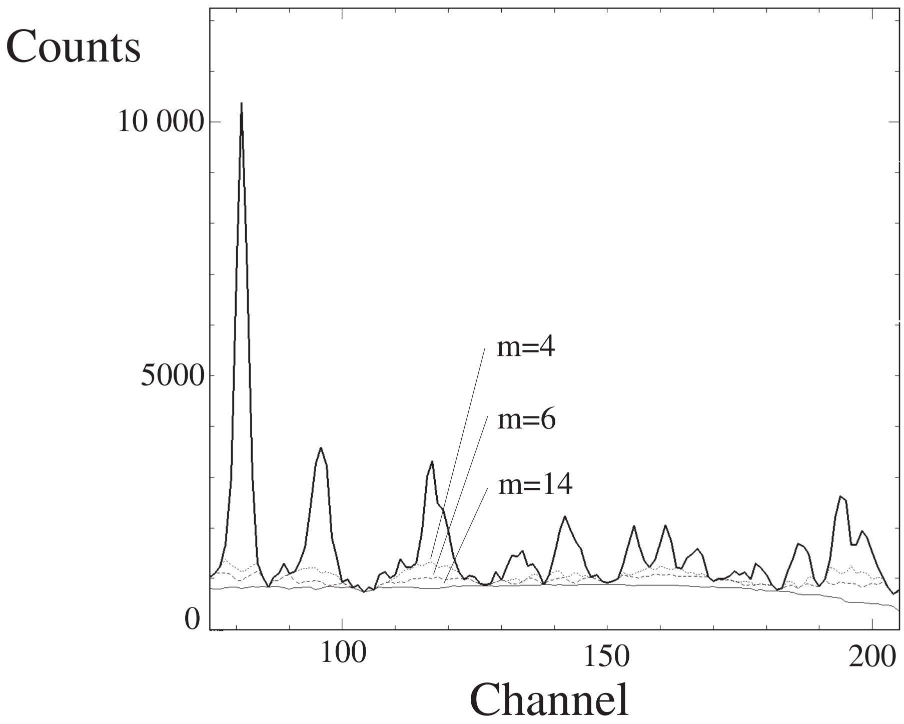

Fig.19 Illustration of the influence of m parameter ($m = 4, 6, 14$) on the estimated background shape.

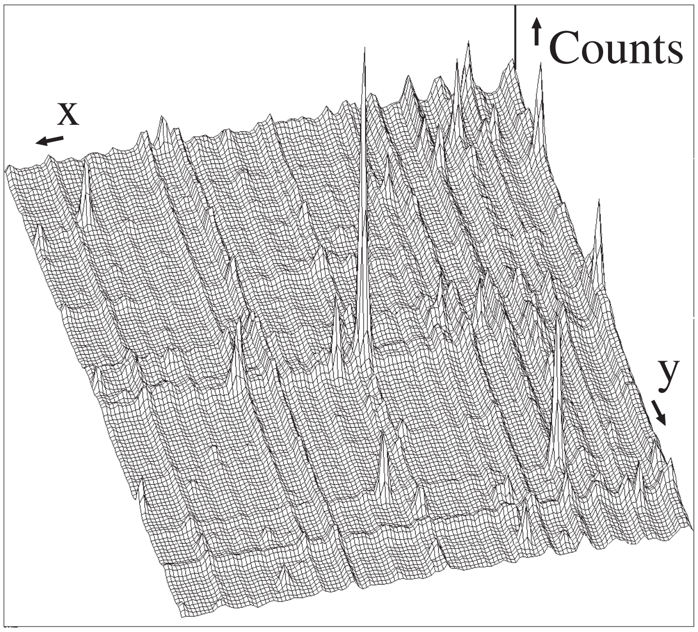

Fig.20 An example of $\gamma - \gamma$ ray spectrum (256x256 channels).

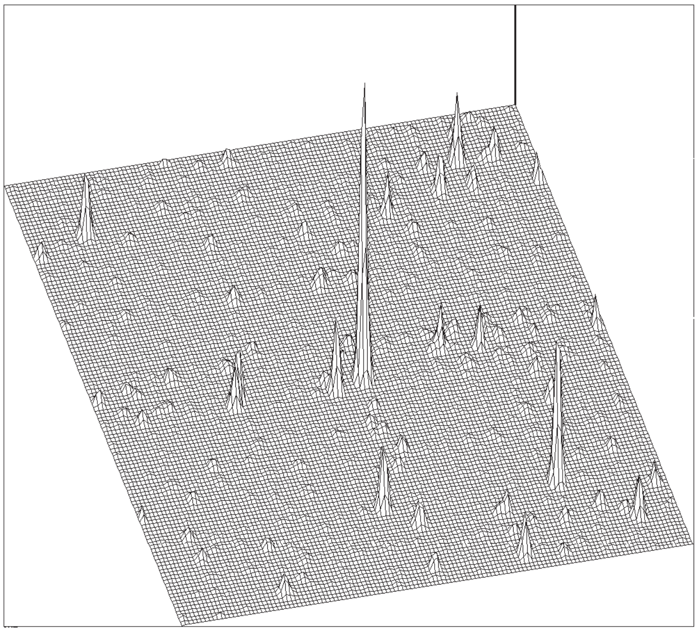

Fig.21 Spectrum from Fig. 20 after background elimination with $m = 8$.

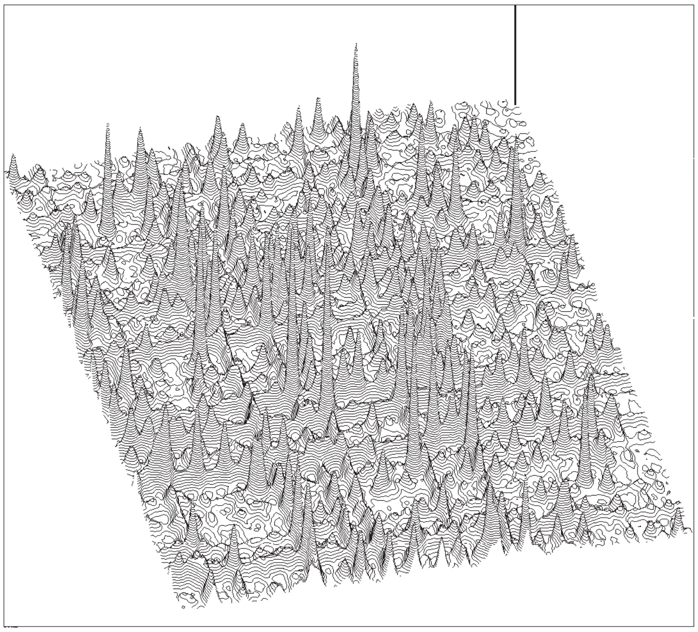

Fig.22 An example of $\gamma - \gamma$ ray spectrum (256x256 channels).

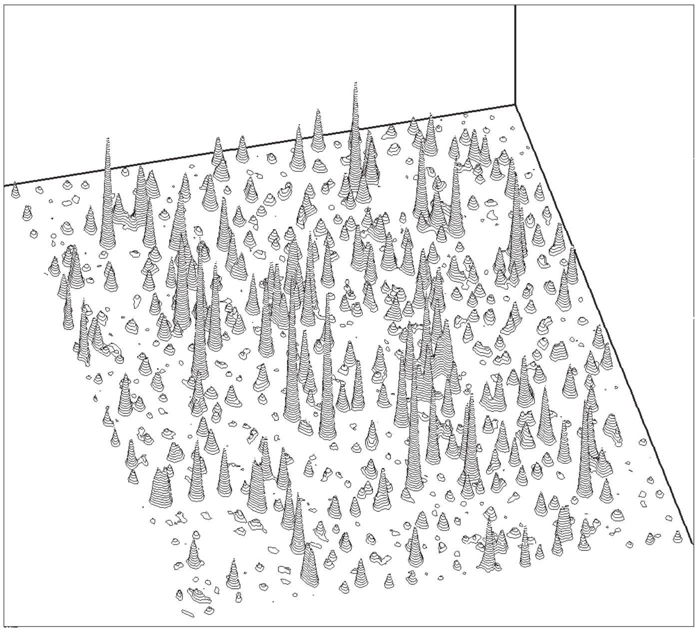

Fig.23 Spectrum from Fig. 22 after background elimination with $m = 8$.

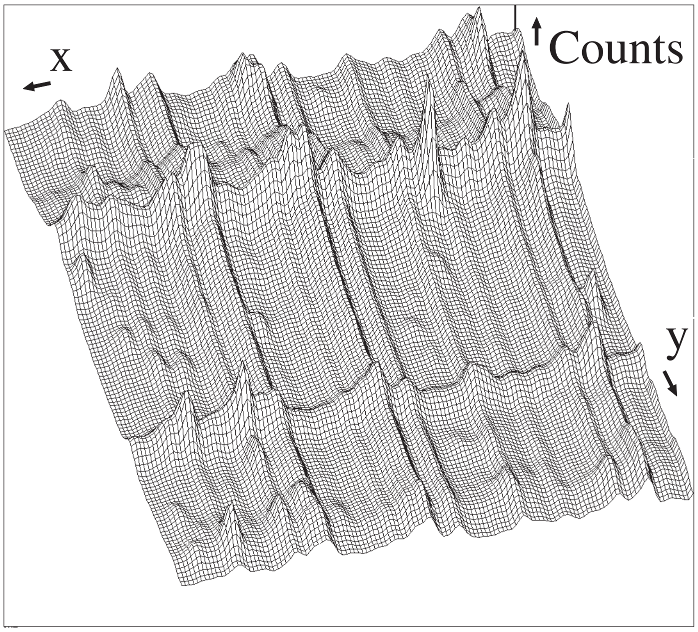

Fig.24 An example of $\gamma - X$-ray spectrum (256x256 channels) with asymmetrical peaks.

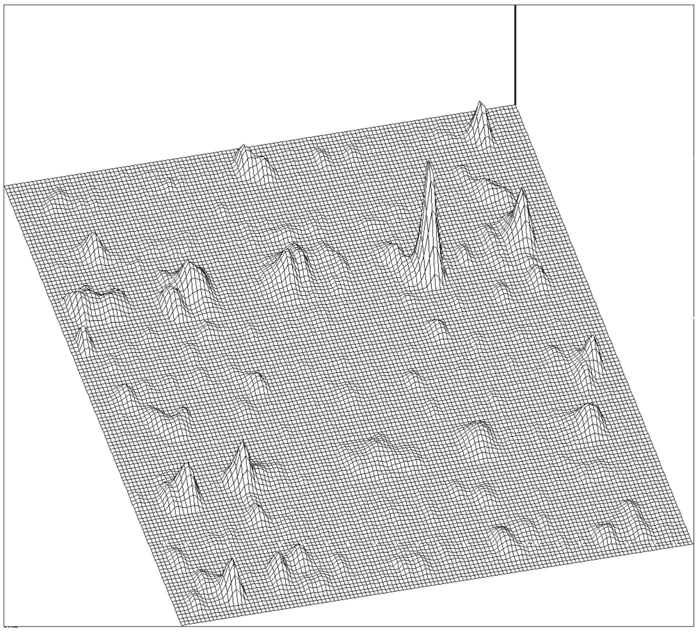

Fig.25 Spectrum from Fig. 24 after background elimination with $m = 20$.

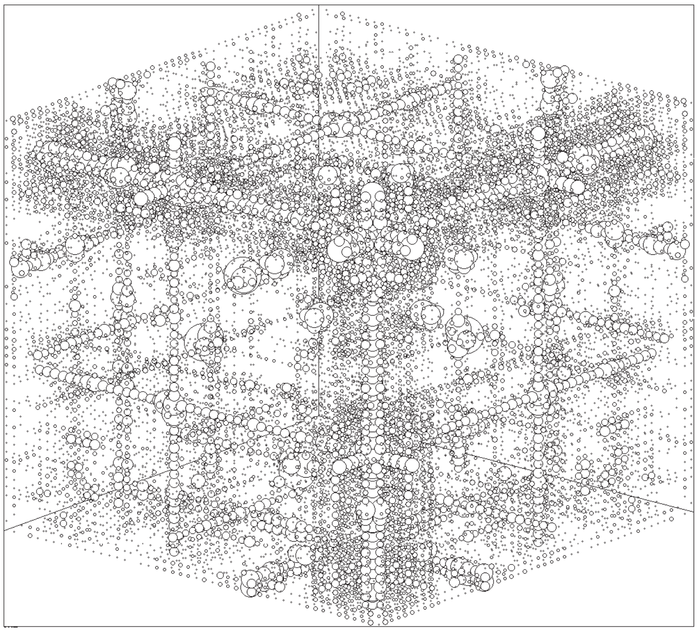

Fig.26 An example of $\gamma - \gamma - \gamma$ ray spectrum (64x64x64 channels). Channels are shown as spheres with diameter proportional to counts they contain.

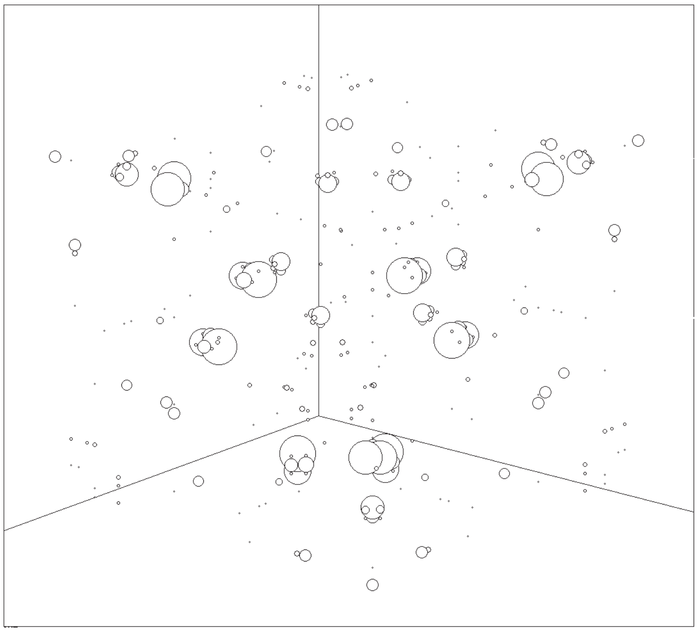

Fig.27 Three dimensional spectrum from Fig. 26 after background elimination with $m = 5$.

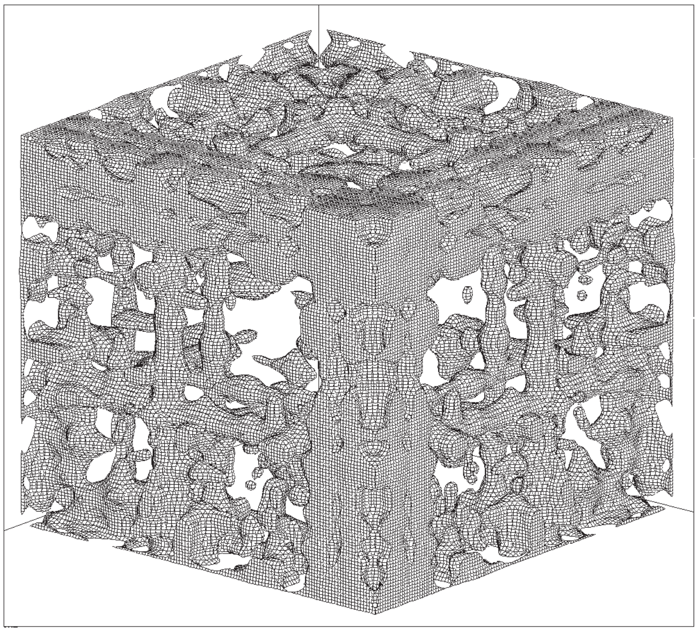

Fig.28 Three dimensional spectrum from Fig. 26 shown in isosurface display mode.

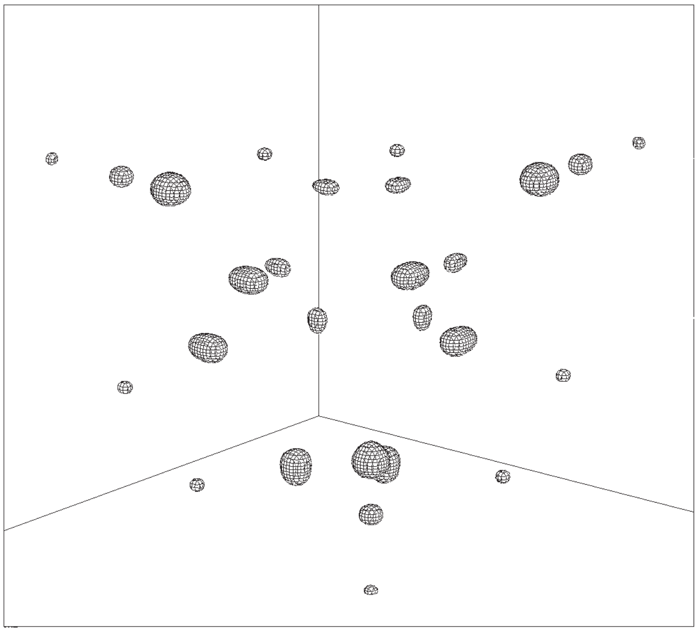

Fig.29 Three dimensional spectrum from Fig. 28 after background elimination ($m = 5$) shown in isosurface display mode.

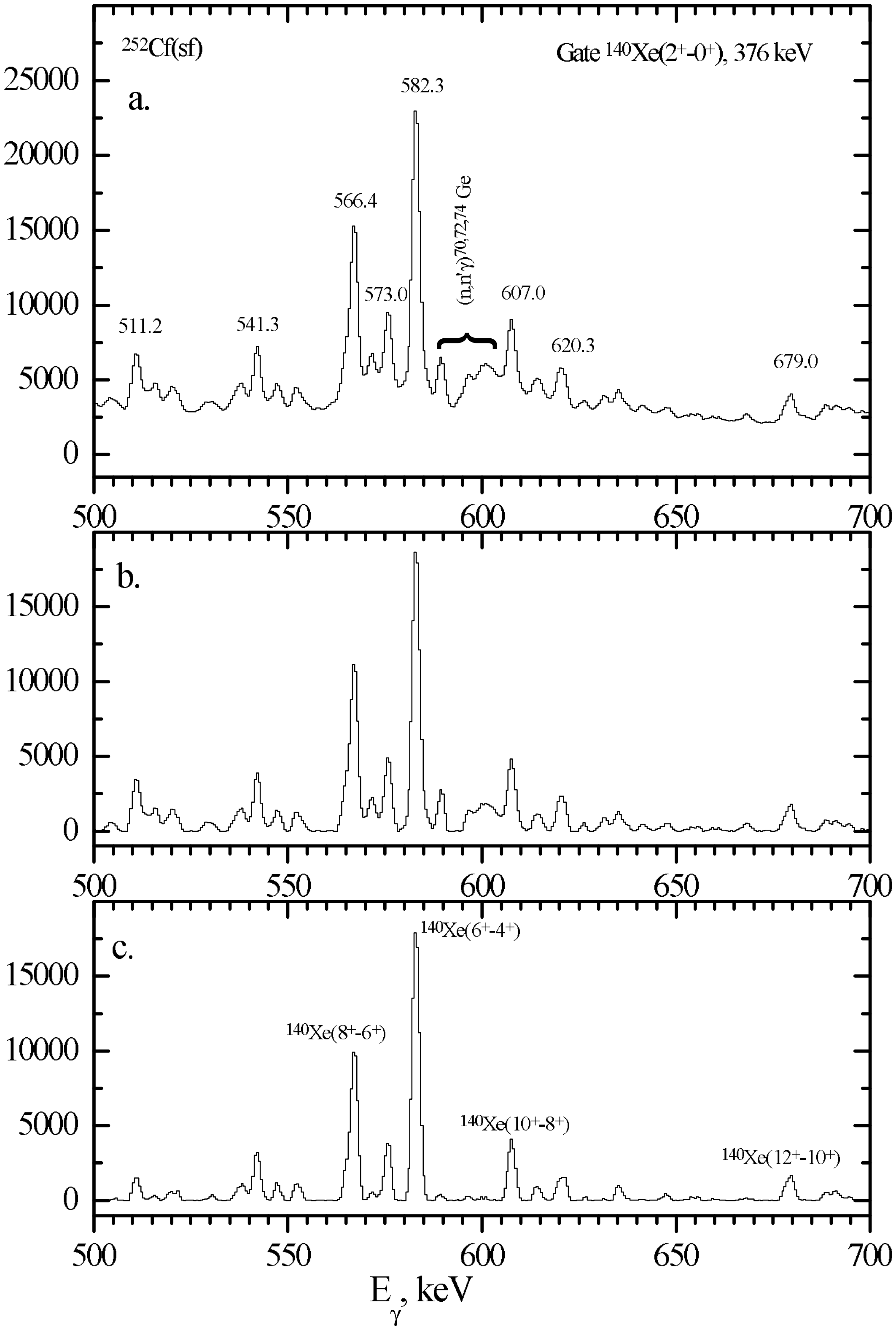

Fig.30 Coincidence spectra from single gated two-fold data showing transitions in ^{104}Xe and Ru isotopes accompanying fission fragment pairs (a) without background elimination, (b) after one dimensional background elimination from (a) and (c) after two dimensional background elimination in two-fold $\gamma-\gamma$ coincidence matrix.

Table captions:

1. Coordinates of points of the class1 for n=4
2. Coordinates of points of the class 2 for n=4

Table 1: Coordinates of points of the class1 for n=4

+	+	+	0	+	+	0	+	+	0	+	+	0	+	+	+
+	+	-	0	+	+	0	-	+	0	+	-	0	+	+	-
+	-	+	0	+	-	0	-	+	0	-	+	0	+	-	+
+	-	-	0	+	-	0	-	+	0	-	-	0	+	-	-
-	+	+	0	-	+	0	+	-	0	+	+	0	-	+	+
-	+	-	0	-	+	0	-	-	0	+	-	0	-	+	-
-	-	+	0	-	-	0	+	-	0	-	+	0	-	-	+
-	-	-	0	-	-	0	-	-	0	-	-	0	-	-	-

Table 2: Coordinates of points of the class 2 for n=4

$++00$	$+0+0$	$+00+$	$0++0$	$0+0+$	$00++$
$+-00$	$+0-0$	$+00-$	$0+-0$	$0+0-$	$00+-$
$-+00$	$-0+0$	$-00+$	$0-+0$	$0-0+$	$00-+$
$--00$	$-0-0$	$-00-$	$0--0$	$0-0-$	$00--$